

DR NABI ZORLU (Orcid ID : 0000-0002-2340-6156)

Article type : Original Article

White matter microstructure and connectivity in patients with obsessive compulsive disorder and their unaffected siblings

Short/running title: White matter in OCD patients and their siblings

Nur Dikmeer¹, Lutfullah Besiroglu¹, Maria A. Di Biase^{2,3}, Andrew Zalesky^{3,4}, Meltem I. Kasal¹, Aslıhan Bilge¹, Ercan Durmaz¹, Serap Polat¹, Fazil Gelal⁵, Nabi Zorlu^{1,*}

¹ Department of Psychiatry, Katip Celebi University, Ataturk Education and Research Hospital, Izmir, Turkey

² Psychiatry Neuroimaging Laboratory, Brigham and Women's Hospital, Harvard Medical School, Boston, MA, USA

³ Department of Psychiatry, Melbourne Neuropsychiatry Centre, The University of Melbourne and Melbourne Health, Carlton South, VIC, Australia

This is the author manuscript accepted for publication and has undergone full peer review but has not been through the copyediting, typesetting, pagination and proofreading process, which may lead to differences between this version and the [Version of Record](#). Please cite this article as [doi: 10.1111/ACPS.13241](https://doi.org/10.1111/ACPS.13241)

This article is protected by copyright. All rights reserved

⁴ Department of Biomedical Engineering, The University of Melbourne, Victoria, 3010, Australia

⁵ Department of Radiodiagnostics, Katip Celebi University, Ataturk Education and Research Hospital, Turkey

Correspondence to: Nabi Zorlu

Department of Psychiatry, Katip Celebi University, Ataturk Education and Research Hospital, Izmir, Turkey

Address: E-Mail: zorlunabi@hotmail.com

Acknowledgements:

This work was supported by Research Fund of Izmir Katip Celebi University (Project number: 2016-GAP-TIPF-0024).

Conflict of Interest Statement:

None

Abstract

Objective: We aimed to examine white matter microstructure and connectivity in individuals with obsessive-compulsive disorder (OCD) and their unaffected siblings, relative to healthy controls.

Methods: Diffusion-weighted magnetic resonance imaging (dMRI) scans were acquired in 30 patients with OCD, 21 unaffected siblings and 31 controls. We examined white matter microstructure using measures of fractional anisotropy (FA), radial diffusivity (RD) and axial diffusivity (AD). Structural networks were examined using network-based statistic (NBS).

Results: Compared to controls, OCD patients showed significantly reduced FA and increased RD in clusters traversing the left forceps minor, inferior fronto-occipital fasciculus, anterior thalamic radiation and cingulum. Furthermore, the OCD group displayed significantly weaker connectivity (quantified by the streamline count) compared to controls in the right hemisphere, most notably in edges connecting subcortical structures to temporo-occipital cortical regions. The sibling group showed intermediate streamline counts, FA and RD values between OCD and healthy control groups in connections found to be abnormal in patients with OCD. However, these reductions did not significantly differ compared to controls.

Conclusion: Therefore, siblings of OCD patients display intermediate levels in dMRI measures of microstructure and connectivity, suggesting white matter abnormalities might be related to the familial predisposition for OCD.

Keywords: 1. Endophenotype, 2. Obsessive-compulsive disorder, 3. Neuroimaging

Significant Outcomes

- OCD patients showed reduced fractional anisotropy (FA) and increased radial diffusivity (RD) in cortico-striato-thalamo-cortical (CSTC) circuit than controls.
- OCD patients showed lower streamline counts in visual pathways than controls.
- Sibling group showed intermediate levels between OCD and HC groups with regard to FA, RD and streamline counts.

Limitations

- Cross-sectional nature of the study.
- Most patients were taking psychotropic medication.

Data availability statement:

- The data of the study will be shared on reasonable request.

Introduction

Obsessive-compulsive disorder (OCD) has a lifetime prevalence of around 2.3% in adults (1) and can be severe and chronic. However, neurobiological mechanisms underlying the disorder remain unclear. First-degree relatives of patients with OCD are at greater risk of developing the disorder, and heritability of OCD is estimated at 42–52% (2, 3), suggesting a large familial component to the disorder. Therefore, the

investigation of unaffected first-degree relatives, in addition to OCD patients and healthy controls, may help to distinguish biomarkers of genetic risk without the confounding effects of the burden of illness, medication or clinical state.

Diffusion-weighted magnetic resonance imaging (dMRI) is a widely used neuroimaging technique to investigate white matter (WM) microstructure in psychiatric disorders. The majority of studies investigating WM with this modality have used a measure known as fractional anisotropy (FA), which provides a general index of WM integrity (4). Demyelination or damage to WM results in more isotropic water movement and manifests in lower FA values. To differentiate myelin-related pathology from axonal damage, the component measures from which FA is derived can be studied: an increase in radial diffusivity (RD) may signify increased space between fibers suggesting demyelination or dysmyelination (5), whereas a decrease in axial diffusivity (AD) may suggest axonal injury (6). Although results are mixed, most previous dMRI studies have reported lower FA in patients with OCD as compared to healthy controls, most consistently in the cingulum bundle (7-13) and corpus callosum (8, 10, 11, 14-18). A small number of previous dMRI studies have also investigated RD and AD in OCD patients, which report higher RD values in the forceps major (19), corpus callosum (14, 20) and in widespread WM (21), as well as no between-group difference in AD, suggesting that decreased myelination rather than axonal degeneration may underlie WM pathology in OCD. However, whether these myelin-linked alterations are state or trait dependent remains unclear.

Few previous studies have examined WM abnormalities in unaffected relatives of patients with OCD. The first such study restricted their analysis to brain regions that were found to be abnormal in OCD patients, and reported reduced FA in the right inferior parietal WM and increased FA in the right medial frontal region in unaffected relatives of OCD patients compared to controls (22). The second study used a whole-brain approach and found reduced FA in the arcuate fibers near the superior parietal lobule and anterior limb of internal capsule in siblings compared to controls (23). A subsequent region-of-interest (ROI) analysis revealed lower FA and increased RD in the

left cingulum bundle in siblings compared to controls (12). While these studies provide the first evidence of WM alterations in relatives of individuals with OCD, the voxel-wise or brain regional approach can limit the extent to which the findings can be interpreted in terms of whole-brain networks.

Growing evidence suggests that dysconnectivity of brain networks, rather than abnormalities in distinct brain regions, might underlie symptom manifestation in psychiatric disorders (24). The structural connectome is a representation of the whole brain as a network of cortical and subcortical regions (nodes) and WM connections between these regions (edges). The network-based statistic (NBS) (25) can be used to identify connectivity differences in the connectome between groups of individuals. One previous study has found decreased structural connectivity in patients with OCD comprising orbitofrontal, striatal, insula and temporo-limbic areas (26). Similarly, a recent study reported decreased FA-weighted connection strength among frontal-limbic areas, including the bilateral dorsolateral part and the right medial part of superior frontal gyrus and the left anterior cingulate and paracingulate gyri in patients with OCD (27). However, no previous study has examined possible structural network alterations in relatives of patients with OCD. Given the evidence for WM abnormalities in both individuals with OCD as well as their unaffected relatives, connectomic analysis using structural networks might provide further insight into the mechanisms underlying OCD.

Aims of the Study

In this study, we aimed to investigate WM integrity and structural connectivity in patients with OCD, their unaffected siblings and controls. We hypothesized that patients with OCD would show lower FA, higher RD and lower structural connectivity compared to the healthy controls, and that siblings display intermediate alterations across these measures.

Material and methods

Subjects

A total of 82 participants (30 patients with OCD, 21 siblings of patients with OCD (13 of whom were related to the assessed OCD patients) and 31 healthy controls (HC)) were enrolled in the study. Exclusion criteria for subjects were as follows: (1) any lifetime substance use disorder (except nicotine); (2) current or past history of any serious psychiatric illness, including any psychotic or bipolar disorder, except for OCD in the OCD group; (3) use of psychotropic medication except patients with OCD; (4) current or past history of any significant neurological disorders; (5) history of loss of consciousness for more than 30 minutes; (6) any family history of OCD for HCs; and (7) any severe hepatic, endocrine or renal disease. All subjects were interviewed using the Structured Clinical Interview for DSM-IV Axis I Disorders (28) to exclude participants with past or current comorbid Axis I diagnoses and to confirm the diagnosis of OCD in the clinical group. As depression is a common comorbidity in OCD, patients also performed the Beck Depression Inventory (29) and were only included when their score was 16 or below. In the OCD group, 14 patients with OCD were treated with both antidepressant and antipsychotic medication, 13 patients were treated only with antidepressants and 3 patients were medication free. The groups were matched for age, sex, education level and packs per year of cigarette smoking. Beck Depression Inventory scores were under the cut-off of 16 in the OCD group (mean \pm SD; 9.1 \pm 3.8). OCD severity was rated with the Dimensional Yale–Brown Obsessive–Compulsive Scale (DY-BOCS) (30). Table 1 shows the demographics and clinical data.

All subjects gave written informed consent to participate in the study. The study was approved by local research and ethics committees.

MRI acquisition

Magnetic resonance imaging was performed using a 1.5 T MR system (GE SignaHDxt, General Electric Medical Systems, Milwaukee, WI, USA). Imaging parameters for T1-weighted structural scan were: TR = 10.7ms, TE = 4.3 ms, matrix = 256 x 256, number of slices = 176, FOV = 256 x 256 mm², NEX = 1, slice thickness = 1 mm. The voxels were therefore isotropic with a size of 1 mm³. All scans were inspected to check for motion artifacts and to rule out gross neuropathology. Diffusion imaging data were acquired in 40 diffusion gradient directions (b-value = 1000 seconds/mm²) and two b = 0 volumes with reversed phase-encoding (right > left and left > right) (repetition time = 6500 ms, echo time = 90 ms, voxel size = 2.1 × 2.1 × 2.1 mm³).

dMRI analysis

As described elsewhere (31), dMRI data were analyzed using the Oxford Centre for Functional MRI of the Brain (FMRIB) Diffusion Toolbox, which is part of FSL (FMRIB Software Library) (32). Data were collected with reversed phase-encode blips, resulting in pairs of images with distortions in opposite directions. The susceptibility-induced off-resonance field was estimated from these image pairs (33) and the two images were combined into a single corrected one. Subsequently, motion and eddy current artefacts were corrected using Eddy (34). A brain mask of the non-diffusion-weighted image was created using the Brain Extraction Tool (35). The diffusion tensor was then calculated with DTIFIT to yield voxel-wise FA, AD and RD maps, which were used in subsequent analyses. The FA images of each subject were then nonlinearly registered to the FMRIB58_FA template using FNIRT. The nonlinear warp was initialized with an affine registration generated with FLIRT (36). The resultant warping transformations were used to resample the FA, AD and RD images into the FMRIB58_FA space. This resampling step was implemented with Applywarp. For voxel-based analyses, the FA, RD and AD maps were smoothed with an isotropic Gaussian kernel with full-width half-maximum of approximately 5mm. The smoothed images of all subjects were merged into 4D volumes, separately for FA, RD and AD.

Mapping of structural brain networks

Whole-brain streamline counts were generated using Mrtrix3 (37). Denoising (38), Gibbs ringing removal (39), motion and distortion correction (34) and bias field correction (40) were performed in the preprocessing steps. The single-fibre WM response function was estimated using the tournier algorithm (41). Single tissue constrained spherical deconvolution (CSD) was used to estimate fibre orientation distributions (42). A total of 50 million probabilistic streamlines were generated using anatomically constrained probabilistic fiber tracking (43) for each subject with a length of 10–250 mm, step size of 1 mm and FOD amplitude threshold of 0.1. The SIFT algorithm was also applied to reduce the overall streamline count to 5 million streamlines (44), with consideration given to recent recommendations (45). Network nodes were based on the 90 cortical and subcortical regions comprising the automated anatomical labeling (AAL) atlas (46). Each element of the connectivity matrix was populated with the log-transformed number of streamlines between the corresponding pair of regions (streamline count), which served as a measure of inter-regional connection strength.

Following a previous study in OCD patients (26), any pairs of regions that were interconnected by one or more streamlines in at least 60% for each group were retained while others were set to zero in each group. Then, edges that were present in at least 60% of the all subjects were retained. This resulted in a connection density of approximately 22%. The stability of results was checked using different threshold levels of 30% and 90%.

Statistical analysis of differences between groups

We first compared whole-brain FA, AD and RD values between OCD and HC groups using a permutation-based parametric inference method (randomise tool in FSL) (47). Corrections for multiple comparisons were performed with an initial cluster forming threshold of $t = 2.3$ (10000 permutations). Statistical testing was constrained to voxels comprising a liberal white matter mask. Age, sex and years of education were included as a nuisance covariates in all analyses. Subsequently, for each cluster of voxels

associated with a significant between group difference, cluster-averaged values of dMRI metrics were extracted for each individual, including those from the sibling group. Cluster-averaged dMRI metrics were compared between the sibling and HC groups using independent samples t-tests.

Connection strengths (log-transformed streamline counts) between OCD and HC groups were compared using the network-based statistic (NBS) (25). The NBS localizes differences in connection strengths to specific networks, while controlling the family-wise error (FWE). The primary threshold for the NBS was set to a t-statistic threshold of 3.1 (10000 permutations). Use of the NBS for inference on brain networks mapped with tractography has been described elsewhere (48). Again, age, sex and years of education were included as a nuisance covariates. Akin to the post-hoc dMRI metric analyses, streamline counts were extracted from significant edges for each individual and compared between sibling and HCs using independent samples t-tests.

Results

Participants characteristics

The groups were matched on age, sex and education level (Table 1).

**** Table 1 ****

dMRI metrics

OCD vs HC

Compared to HC group, patients with OCD showed lower FA in a single cluster (MNI-coordinates: $x = 102$, $y = 159$, $z = 60$, cluster size = 3534 voxels, $p = 0.033$) within the left forceps minor, inferior fronto-occipital fasciculus (IFOF), anterior thalamic radiation (ATR) and cingulum (Fig. 1A, Table 2). The OCD group displayed significantly higher RD values compared to the HC group in one cluster which was in brain regions (MNI-coordinates: $x = 106$, $y = 162$, $z = 57$, cluster size = 3094 voxels, $p = 0.049$) overlapping with cluster of reduced FA in OCD patients (Fig. 1B, Table 2). AD values did not significantly differ between OCD and HC groups.

Sibling vs HC

Mean FA and RD values were extracted from significant voxelwise clusters to examine group differences between the sibling and HC groups. Cluster-averaged FA and RD in the sibling group was positioned in between the values for the HC and OCD groups. However, cluster-averaged FA and RD did not significantly differ between sibling and HC groups (Fig. 1C, Fig. 1D, and Table 2). Furthermore, no significant differences between the sibling and HC groups were found within the white matter mask.

**** Figure 1 and Table 2 ****

Structural Connectivity

OCD vs HC

The NBS identified a single network of significantly lower streamline counts in patients with OCD compared to HCs ($p = 0.026$). The network contained 9 nodes connected by 8 edges and was right localized. These connections linked the caudate nucleus with the calcarine, middle occipital and superior and middle temporal cortex. Another two edges linked the thalamus with the cuneus and middle occipital cortex. Another two edges linked the calcarine to the inferior occipital cortex and pallidum with the middle occipital cortex (Fig. 2A, Table 3). Together, these results indicate lower structural connectivity in right ventral visual pathways (49, 50) in OCD. No edges showed higher streamline counts in OCD patients compared to HC.

The connectivity results were stable at a streamline threshold of 30%. Specifically, NBS identified a significant cluster of lower streamline counts in patients with OCD compared to controls, which yielded one additional edge (more than the main analysis) that linked the right calcarine to the right pallidum ($p = 0.029$) (Table S1). Four edges remained significant ($p = 0.020$) but four edges (right caudate to right calcarine, right thalamus to right cuneus, right pallidum to right middle occipital and right calcarine to right inferior occipital) lost their significance at threshold of 90% (Table S2).

Sibling vs HC

Mean log-transformed streamline counts were extracted from significant edges for posthoc analyses comparing the sibling and HC groups. The sibling group showed intermediate streamline counts between HC and OCD groups across all edges. In two of these edges, siblings displayed significantly lower streamline counts compared to HCs, which linked the caudate nucleus with the calcarine ($p = 0.043$) and thalamus with the cuneus ($p = 0.019$) (Fig. 2B, Fig. 2C, Table 3 and Fig. S1). However, these differences did not remain significant after FDR correction for multiple comparisons (across the eight connections).

Exploratory whole-brain analysis revealed no significant differences between sibling and HC groups.

**** Figure 2 and Table 3 ****

Correlation analysis

Spearman's correlation analysis was used to test for relationships between significant dMRI metric values and streamline counts with symptom severity (DY-BOCS total score) within the OCD group. No significant correlations were detected between DY-BOCS total score and significant dMRI metrics values or streamline counts.

Discussion

In the current study, we examined patients with OCD, unaffected siblings of OCD patients and healthy controls in order to identify alterations in WM microstructure and connectivity that may be associated with the familial risk for OCD. We found lower WM anisotropy in the left hemisphere involving the limbic pathways (i.e., cingulum and ATR) and cortico-cortical association tracts (i.e., IFOF), as well as in interhemispheric tracts

(i.e., forceps minor of the corpus callosum) in OCD patients compared to the HC group. Increased RD in the absence of AD changes in the OCD group might indicate a role for reduced myelination in the microstructural changes observed in this group. At the network level, OCD patients showed decreased structural connectivity in edges connecting subcortical structures, specifically caudate nucleus, thalamus and pallidum to temporo-occipital cortical regions within the right ventral visual pathways. Furthermore, although not significant, the sibling group showed intermediate levels between OCD and HC groups with regard to FA, RD and streamline counts in connections found to be abnormal in patients with OCD.

Compared to HCs, the OCD group showed lower FA and higher RD values in the anterior cingulum, forceps minor and ATR, which is in line with the classical cortico-striato-thalamo-cortical (CSTC) circuit model of OCD (10, 51-53) and with prior research in this area. Specifically, reduced FA was previously reported in OCD patients within the anterior cingulum bundle (7, 9-11, 13, 51, 54), the forceps minor (8, 10, 11, 14, 16-18, 20) and the ATR (21, 55). However, we also observed alterations outside the CSTC, including within the IFOF, which connects the frontal lobe to parieto-occipito-temporal regions. Thus, our results suggest that microstructural abnormalities in OCD may be more widespread than previously thought.

In addition to microstructural alterations in WM, OCD patients also showed reduced structural connectivity (i.e., streamline counts) compared to healthy controls, between the right caudate nucleus and right temporo-occipital regions and also between the right thalamus and right occipital regions. These findings are in contrast to previous studies using a network-based approach (26, 27). Specifically, Reess et al. (2016) observed decreased structural connectivity in patients with OCD, involving orbitofrontal, striatal, insula and temporo-limbic areas (26); and, Qin et al. (2019) reported reduced FA-weighted structural connectivity between the right superior frontal gyrus and left anterior cingulate gyrus (27). One possible explanation for the mixed findings with regard to the specific connections/subnetworks involved might relate to methodological differences between the studies. For example, we used probabilistic tractography to estimate

structural connectivity, while the two previous studies used a deterministic approach. A previous study reported that probabilistic approaches are superior compared to deterministic tractography in determining visual pathways, which were implicated in the subnetwork identified by our study (56). In addition, Reess et al. (2016) used a different parcellation scheme to construct the connectivity matrix (26) and differences in tractography methods and parcellation schemes have been shown to affect connectome reconstruction (57).

Inconsistencies between our study and previous studies with regard to the spatial location of connectivity deficits in OCD may also be sample-related. Our study included patients with OCD that were mostly treated with psychotropic medications including antipsychotics and different classes of antidepressants, while previous studies included mostly SSRI treated (26) or medication-free patients (27). Indeed, previous studies reported an increase in the FA following antipsychotic (58) or antidepressant treatment (59) including within fronto-striatal structures, which might explain why our structural connectivity findings were constrained to visual pathways. Interestingly, our results were more in line with previous connectivity studies using resting-state functional imaging in patients with OCD. For example, functional connectivity alterations in OCD has been found between the caudate and temporo-occipital regions (60-62) and between the thalamus and occipital cortex (63-65). Speculatively, our findings of reduced structural connectivity between occipital and subcortical structures might be associated with visuospatial deficits, which are observed in patients with OCD (66-70). Given that OCD symptoms are heterogeneous across patients (71), it is possible that our sample contained a greater portion of patients with severe visuospatial deficits, compared to samples from previous structural connectivity studies.

White matter alterations in siblings

The sibling group showed intermediate FA and RD values between OCD and HC groups in the cingulum and forceps minor which are spatially in line with previous studies reporting intermediate FA values in the medial frontal regions (22) and

intermediate FA and RD values in cingulum (12) in unaffected siblings of OCD patients. Furthermore, the sibling group also showed intermediate streamline numbers in all edges with significantly lower streamline counts in patients with OCD compared to HCs. It is notable that while streamline counts were lower in sibling compared to HCs (falling between OCD and HC groups), these reductions were not significant. It is possible that intermediate levels might be due to lower expression of high-risk genes in the siblings compared to the OCDs, but future studies investigating larger sample sizes are needed to formally test this hypothesis.

Increased radial diffusivity in patients with OCD

Consistent with previous studies (12, 14, 19, 20), FA differences were mainly due to increases in RD values in both OCD and sibling groups suggesting myelin-related WM alterations. In line with this hypothesis, a recent longitudinal study in healthy adolescents and young adults reported increased compulsivity is tied to slower myelination in frontostriatal regions (72). Although the mechanisms underlying myelin-related abnormalities in OCD are still unknown, previous studies have implicated myelin-related genes in OCD, such as oligodendrocyte lineage transcription factor 2 (OLIG2) (73-75) and myelin oligodendrocyte glycoprotein (MOG) (76). OCD is further linked to genetic variants related to glutamatergic, dopaminergic, and neurodevelopmental pathways that influence neural circuit establishment (77). Thus, genetic factors may contribute to myelin-related WM abnormalities in OCD and could further underlie the increase we observed in RD values.

The current study has several potential limitations. The most obvious is the cross-sectional nature of the study. Thus, potential differential changes in WM abnormalities over the course of illness in OCD remain to be directly established. Second, our sample was relatively small, which limits power for detecting between-group comparisons. Third, the field strength of 1.5 Tesla should be noted. Fourth, although similar to previous studies within clinical populations, our acquisition protocol (40 diffusion gradient directions at a b-value of 1000 s/mm²) was not ideally suited to CSD (78).

However, it has been shown that CSD outperforms classical diffusion tensor model for datasets acquired with comparable protocols (79). Fifth, recent work indicates that the SIFT method can potentially lead to erroneous inference when applied to pathological connectomes (45). Future methodological work should focus on investigating the impact of streamline filters on structural connectomes mapped in psychiatric cohorts. Sixth, dMRI is an intrinsically noise-sensitive and low-resolution technique which has limited capacity to resolve crossing, converging or diverging fibers and the neurobiological meaning of dMRI metrics remains unclear (80). In addition, symptom severity was assessed within the patient group only using the DY-BOCS, and thus we may have underestimated subclinical symptoms within the sibling and HC groups. Finally, most patients were taking psychotropic medication, however detailed medication information was not available for this study. Structural and functional alterations have been reported following psychotropic medication in patients with OCD (81, 82). Therefore, we could not reliably disentangle effects of medication on dMRI metrics and structural connectivity within the OCD group.

In conclusion, this is the first study to examine WM structural networks in unaffected siblings of patients with OCD. While OCD patients displayed WM connectivity deficits in a widespread network of brain regions connecting temporo-occipital cortical regions and subcortical structures, their unaffected siblings displayed intermediate decline as compared to controls, suggesting that WM abnormalities in both microstructure and connectivity relate to familial predisposition for OCD.

References

1. RUSCIO AM, STEIN DJ, CHIU WT, KESSLER RC. The epidemiology of obsessive-compulsive disorder in the National Comorbidity Survey Replication. *Mol Psychiatry* 2010;15:53-63.
2. MATAIX-COLS D, BOMAN M, MONZANI B, et al. Population-based, multigenerational family clustering study of obsessive-compulsive disorder. *JAMA Psychiatry* 2013;70:709-717.

3. PAULS DL, ABRAMOVITCH A, RAUCH SL, GELLER DA. Obsessive-compulsive disorder: an integrative genetic and neurobiological perspective. *Nat Rev Neurosci* 2014;15:410-424.
4. KUBICKI M, WESTIN CF, MAIER SE, et al. Diffusion Tensor Imaging and Its Application to Neuropsychiatric Disorders. *Harvard Review of Psychiatry* 2002;10:324-336.
5. HARSAN LA, POULET P, GUIGNARD B, et al. Brain dysmyelination and recovery assessment by noninvasive in vivo diffusion tensor magnetic resonance imaging. *J Neurosci Res* 2006;83:392-402.
6. LAZAR M, WEINSTEIN DM, TSURUDA JS, et al. White matter tractography using diffusion tensor deflection. *Human brain mapping* 2003;18:306-321.
7. VERSACE A, GRAUR S, GREENBERG T, et al. Reduced focal fiber collinearity in the cingulum bundle in adults with obsessive-compulsive disorder. *Neuropsychopharmacology* 2019;44:1182-1188.
8. NAKAMAE T, NARUMOTO J, SAKAI Y, et al. Diffusion tensor imaging and tract-based spatial statistics in obsessive-compulsive disorder. *J Psychiatr Res* 2011;45:687-690.
9. BENEDETTI F, GIACOSA C, RADAELLI D, et al. Widespread changes of white matter microstructure in obsessive-compulsive disorder: effect of drug status. *Eur Neuropsychopharmacol* 2013;23:581-593.
10. KOCH K, REESS TJ, RUS OG, ZIMMER C, ZAUDIG M. Diffusion tensor imaging (DTI) studies in patients with obsessive-compulsive disorder (OCD): a review. *J Psychiatr Res* 2014;54:26-35.
11. RADUA J, GRAU M, VAN DEN HEUVEL OA, et al. Multimodal voxel-based meta-analysis of white matter abnormalities in obsessive-compulsive disorder. *Neuropsychopharmacology* 2014;39:1547-1557.
12. FAN S, VAN DEN HEUVEL OA, CATH DC, et al. Mild white matter changes in un-medicated obsessive-compulsive disorder patients and their unaffected siblings. *Frontiers in neuroscience* 2016;9:495.

13. DE SALLES ANDRADE JB, FERREIRA FM, SUO C, et al. An MRI Study of the Metabolic and Structural Abnormalities in Obsessive-Compulsive Disorder. *Front Hum Neurosci* 2019;13:186.
14. BORA E, HARRISON BJ, FORNITO A, et al. White matter microstructure in patients with obsessive-compulsive disorder. *J Psychiatry Neurosci* 2011;36:42-46.
15. FONTENELLE LF, BRAMATI IE, MOLL J, MENDLOWICZ MV, DE OLIVEIRA-SOUZA R, TOVAR-MOLL F. White Matter Changes in OCD Revealed by Diffusion Tensor Imaging. *CNS Spectr* 2011;16:101-109.
16. ZHOU C, XU J, PING L, et al. Cortical thickness and white matter integrity abnormalities in obsessive-compulsive disorder: A combined multimodal surface-based morphometry and tract-based spatial statistics study. *Depress Anxiety* 2018;35:742-751.
17. HE X, STEINBERG E, STEFAN M, FONTAINE M, SIMPSON HB, MARSH R. Altered frontal interhemispheric and fronto-limbic structural connectivity in unmedicated adults with obsessive-compulsive disorder. *Hum Brain Mapp* 2018;39:803-810.
18. HARTMANN T, VANDBORG S, ROSENBERG R, SØRENSEN L, VIDEBECH P. Increased fractional anisotropy in cerebellum in obsessive-compulsive disorder. *Acta neuropsychiatrica* 2016;28:141-148.
19. WATANABE A, NAKAMAE T, SAKAI Y, et al. The detection of white matter alterations in obsessive-compulsive disorder revealed by TRActs Constrained by UnderLying Anatomy (TRACULA). *Neuropsychiatr Dis Treat* 2018;14:1635-1643.
20. GAN J, ZHONG M, FAN J, et al. Abnormal white matter structural connectivity in adults with obsessive-compulsive disorder. *Transl Psychiatry* 2017;7:e1062.
21. BOLLETTINI I, MAZZA MG, MUZZARELLI L, et al. White matter alterations associate with onset symptom dimension in obsessive-compulsive disorder. *Psychiatry Clin Neurosci* 2018;72:13-27.
22. MENZIES L, WILLIAMS GB, CHAMBERLAIN SR, et al. White matter abnormalities in patients with obsessive-compulsive disorder and their first-degree relatives. *Am J Psychiatry* 2008;165:1308-1315.

23. PENG Z, SHI F, SHI C, et al. Structural and diffusion property alterations in unaffected siblings of patients with obsessive-compulsive disorder. *PLoS One* 2014;9:e85663.
24. FORNITO A, BULLMORE ET, ZALESKY A. Opportunities and Challenges for Psychiatry in the Connectomic Era. *Biol Psychiatry Cogn Neurosci Neuroimaging* 2017;2:9-19.
25. ZALESKY A, FORNITO A, BULLMORE ET. Network-based statistic: identifying differences in brain networks. *Neuroimage* 2010;53:1197-1207.
26. REESS TJ, RUS OG, SCHMIDT R, et al. Connectomics-based structural network alterations in obsessive-compulsive disorder. *Transl Psychiatry* 2016;6:e882.
27. QIN J, SUI J, NI H, et al. The shared and distinct white matter networks between drug-naive patients with obsessive-compulsive disorder and schizophrenia. *Frontiers in neuroscience* 2019;13:96.
28. FIRST MB, SPITZER RL, GIBBON M, WILLIAMS JBW. Structured Clinical Interview for DSM-IV Axis I Disorders (SCID-I), Clinician Version: Administration Booklet. American Psychiatric Association Publishing; 1996.
29. BECK AT, STEER RA, CARBIN MG. Psychometric properties of the Beck Depression Inventory: Twenty-five years of evaluation. *Clinical psychology review* 1988;8:77-100.
30. ROSARIO-CAMPOS MC, MIGUEL EC, QUATRANO S, et al. The Dimensional Yale-Brown Obsessive-Compulsive Scale (DY-BOCS): an instrument for assessing obsessive-compulsive symptom dimensions. *Mol Psychiatry* 2006;11:495-504.
31. ZORLU N, ANGELIQUE DI BIASE M, KALAYCI CC, et al. Abnormal white matter integrity in synthetic cannabinoid users. *Eur Neuropsychopharmacol* 2016;26:1818-1825.
32. SMITH SM, JENKINSON M, WOOLRICH MW, et al. Advances in functional and structural MR image analysis and implementation as FSL. *Neuroimage* 2004;23 Suppl 1:S208-219.
33. ANDERSSON JL, SKARE S, ASHBURNER J. How to correct susceptibility distortions in spin-echo echo-planar images: application to diffusion tensor imaging. *Neuroimage* 2003;20:870-888.

34. ANDERSSON JL, SOTIROPOULOS SN. An integrated approach to correction for off-resonance effects and subject movement in diffusion MR imaging. *Neuroimage* 2016;125:1063-1078.
35. SMITH SM. Fast robust automated brain extraction. *Hum Brain Mapp* 2002;17:143-155.
36. JENKINSON M, SMITH S. A global optimisation method for robust affine registration of brain images. *Med Image Anal* 2001;5:143-156.
37. TOURNIER JD, SMITH R, RAFFELT D, et al. MRtrix3: A fast, flexible and open software framework for medical image processing and visualisation. *Neuroimage* 2019;202:116137.
38. VERAART J, NOVIKOV DS, CHRISTIAENS D, ADES-ARON B, SIJBERS J, FIEREMANS E. Denoising of diffusion MRI using random matrix theory. *Neuroimage* 2016;142:394-406.
39. KELLNER E, DHITAL B, KISELEV VG, REISERT M. Gibbs-ringing artifact removal based on local subvoxel-shifts. *Magn Reson Med* 2016;76:1574-1581.
40. TUSTISON NJ, AVANTS BB, COOK PA, et al. N4ITK: improved N3 bias correction. *IEEE transactions on medical imaging* 2010;29:1310-1320.
41. TOURNIER JD, CALAMANTE F, CONNELLY A. Determination of the appropriate b value and number of gradient directions for high-angular-resolution diffusion-weighted imaging. *NMR in Biomedicine* 2013;26:1775-1786.
42. TOURNIER JD, CALAMANTE F, CONNELLY A. Robust determination of the fibre orientation distribution in diffusion MRI: non-negativity constrained super-resolved spherical deconvolution. *Neuroimage* 2007;35:1459-1472.
43. SMITH RE, TOURNIER JD, CALAMANTE F, CONNELLY A. Anatomically-constrained tractography: improved diffusion MRI streamlines tractography through effective use of anatomical information. *Neuroimage* 2012;62:1924-1938.
44. SMITH RE, TOURNIER J-D, CALAMANTE F, CONNELLY A. SIFT: Spherical-deconvolution informed filtering of tractograms. *Neuroimage* 2013;67:298-312.
45. ZALESKY A, SARWAR T, RAMAMOHANARAO K. A cautionary note on the use of SIFT in pathological connectomes. *Magn Reson Med* 2020;83:791-794.

46. TZOURIO-MAZOYER N, LANDEAU B, PAPATHANASSIOU D, et al. Automated anatomical labeling of activations in SPM using a macroscopic anatomical parcellation of the MNI MRI single-subject brain. *Neuroimage* 2002;15:273-289.
47. NICHOLS TE, HOLMES AP. Nonparametric permutation tests for functional neuroimaging: a primer with examples. *Hum Brain Mapp* 2002;15:1-25.
48. DI BIASE MA, CROPLEY VL, BAUNE BT, et al. White matter connectivity disruptions in early and chronic schizophrenia. *Psychol Med* 2017;47:2797-2810.
49. SEGER CA. The visual corticostriatal loop through the tail of the caudate: circuitry and function. *Frontiers in systems neuroscience* 2013;7:104.
50. KRAVITZ DJ, SALEEM KS, BAKER CI, UNGERLEIDER LG, MISHKIN M. The ventral visual pathway: an expanded neural framework for the processing of object quality. *Trends in cognitive sciences* 2013;17:26-49.
51. PIRAS F, PIRAS F, CALTAGIRONE C, SPALLETTA G. Brain circuitries of obsessive compulsive disorder: a systematic review and meta-analysis of diffusion tensor imaging studies. *Neurosci Biobehav Rev* 2013;37:2856-2877.
52. ALEXANDER GE, DELONG MR, STRICK PL. Parallel organization of functionally segregated circuits linking basal ganglia and cortex. *Annu Rev Neurosci* 1986;9:357-381.
53. CAVALLARO R, CAVEDINI P, MISTRETTA P, et al. Basal-corticofrontal circuits in schizophrenia and obsessive-compulsive disorder: a controlled, double dissociation study. *Biol Psychiatry*. 2003;54:437-443.
54. HA TH, KANG DH, PARK JS, et al. White matter alterations in male patients with obsessive-compulsive disorder. *Neuroreport* 2009;20:735-739.
55. JENKINS LM, BARBA A, CAMPBELL M, et al. Shared white matter alterations across emotional disorders: A voxel-based meta-analysis of fractional anisotropy. *Neuroimage Clin* 2016;12:1022-1034.
56. LILJA Y, LJUNGBERG M, STARCK G, MALMGREN K, RYDENHAG B, NILSSON DT. Visualizing Meyer's loop: A comparison of deterministic and probabilistic tractography. *Epilepsy Res* 2014;108:481-490.
57. ZALESKY A, FORNITO A, HARDING IH, et al. Whole-brain anatomical networks: does the choice of nodes matter? *Neuroimage* 2010;50:970-983.

58. REIS MARQUES T, TAYLOR H, CHADDOCK C, et al. White matter integrity as a predictor of response to treatment in first episode psychosis. *Brain* 2014;137:172-182.
59. FAN Q, YAN X, WANG J, et al. Abnormalities of white matter microstructure in unmedicated obsessive-compulsive disorder and changes after medication. *PLoS One* 2012;7:e35889.
60. CHEN Y, JUHAS M, GREENSHAW AJ, et al. Abnormal resting-state functional connectivity of the left caudate nucleus in obsessive-compulsive disorder. *Neurosci Lett* 2016;623:57-62.
61. PARK J, KIM T, KIM M, LEE TY, KWON JS. Functional Connectivity of the Striatum as a Neural Correlate of Symptom Severity in Patient with Obsessive-Compulsive Disorder. *Psychiatry Investigation* 2020;17:87.
62. HARRISON BJ, PUJOL J, CARDONER N, et al. Brain corticostriatal systems and the major clinical symptom dimensions of obsessive-compulsive disorder. *Biol Psychiatry* 2013;73:321-328.
63. CHEN Y, MENG Z, ZHANG Z, et al. The right thalamic glutamate level correlates with functional connectivity with right dorsal anterior cingulate cortex/middle occipital gyrus in unmedicated obsessive-compulsive disorder: A combined fMRI and (1)H-MRS study. *Aust N Z J Psychiatry* 2019;53:207-218.
64. LI K, ZHANG H, YANG Y, et al. Abnormal functional network of the thalamic subregions in adult patients with obsessive-compulsive disorder. *Behav Brain Res* 2019;371:111982.
65. MOREIRA PS, MARQUES P, SORIANO-MAS C, et al. The neural correlates of obsessive-compulsive disorder: a multimodal perspective. *Transl Psychiatry* 2017;7:e1224.
66. RAMPACHER F, LENNERTZ L, VOGLEY A, et al. Evidence for specific cognitive deficits in visual information processing in patients with OCD compared to patients with unipolar depression. *Prog Neuropsychopharmacol Biol Psychiatry* 2010;34:984-991.
67. STERN ER, MURATORE AF, TAYLOR SF, ABELSON JL, HOF PR, GOODMAN WK. Switching between internally and externally focused attention in obsessive-

compulsive disorder: Abnormal visual cortex activation and connectivity. *Psychiatry Res Neuroimaging* 2017;265:87-97.

68. SEGALAS C, ALONSO P, LABAD J, et al. Verbal and nonverbal memory processing in patients with obsessive-compulsive disorder: its relationship to clinical variables. *Neuropsychology* 2008;22:262-272.

69. RAO NP, REDDY YC, KUMAR KJ, KANDAVEL T, CHANDRASHEKAR CR. Are neuropsychological deficits trait markers in OCD? *Prog Neuropsychopharmacol Biol Psychiatry* 2008;32:1574-1579.

70. SAVAGE CR, BAER L, KEUTHEN NJ, BROWN HD, RAUCH SL, JENIKE MA. Organizational strategies mediate nonverbal memory impairment in obsessive-compulsive disorder. *Biol Psychiatry* 1999;45:905-916.

71. BLOCH MH, LANDEROS-WEISENBERGER A, ROSARIO MC, PITTENGER C, LECKMAN JF. Meta-analysis of the symptom structure of obsessive-compulsive disorder. *Am J Psychiatry* 2008;165:1532-1542.

72. ZIEGLER G, HAUSER TU, MOUTOUSSIS M, et al. Compulsivity and impulsivity traits linked to attenuated developmental frontostriatal myelination trajectories. *Nature neuroscience* 2019;22:992-999.

73. VIEIRA-FONSECA T, FONTENELLE LF, KOHLRAUSCH FB. OLIG2 gene polymorphisms are associated with nasty, unpleasant and uncontrollable thoughts in obsessive-compulsive disorder. *J Clin Neurosci* 2019;70:202-207.

74. STEWART SE, PLATKO J, FAGERNESS J, et al. A genetic family-based association study of OLIG2 in obsessive-compulsive disorder. *Arch Gen Psychiatry* 2007;64:209-214.

75. ZHANG X, LIU J, GUO Y, JIANG W, YU J. Association study between oligodendrocyte transcription factor 2 gene and obsessive-compulsive disorder In A Chinese Han population. *Depress Anxiety* 2015;32:720-727.

76. ZAI G, BEZCHLIBNYK YB, RICHTER MA, et al. Myelin oligodendrocyte glycoprotein (MOG) gene is associated with obsessive-compulsive disorder. *Am J Med Genet B Neuropsychiatr Genet* 2004;129B:64-68.

77. GASSO P, ORTIZ AE, MAS S, et al. Association between genetic variants related to glutamatergic, dopaminergic and neurodevelopment pathways and white

matter microstructure in child and adolescent patients with obsessive-compulsive disorder. *J Affect Disord* 2015;186:284-292.

78. TOURNIER JD, CALAMANTE F, GADIAN DG, CONNELLY A. Direct estimation of the fiber orientation density function from diffusion-weighted MRI data using spherical deconvolution. *Neuroimage* 2004;23:1176-1185.

79. CALAMUNERI A, ARRIGO A, MORMINA E, et al. White Matter Tissue Quantification at Low b-Values Within Constrained Spherical Deconvolution Framework. *Front Neurol* 2018;9:716.

80. JONES DK, KNOSCHE TR, TURNER R. White matter integrity, fiber count, and other fallacies: the do's and don'ts of diffusion MRI. *Neuroimage* 2013;73:239-254.

81. HOEXTER MQ, DE SOUZA DURAN FL, D'ALCANTE CC, et al. Gray matter volumes in obsessive-compulsive disorder before and after fluoxetine or cognitive-behavior therapy: a randomized clinical trial. *Neuropsychopharmacology* 2012;37:734-745.

82. BEUCKE JC, SEPULCRE J, TALUKDAR T, et al. Abnormally high degree connectivity of the orbitofrontal cortex in obsessive-compulsive disorder. *JAMA Psychiatry* 2013;70:619-629.

Fig. 1 Regions of **A)** reduced fractional anisotropy, **B)** increased radial diffusivity in the OCD group relative to the HC group. Boxplot of **C)** fractional anisotropy and **D)** radial diffusivity values in significant clusters showed significant differences between OCD and HC groups. Group means are demarcated by the “+”. Radial diffusivity: $\times 10^{-3}$ mm²/s.

Fig. 2 A) Lower structural connectivity in patients with OCD compared to HC **B)** and **C)** Bar graphs showing mean streamline counts from edges showed significant differences (uncorrected level) between SIB and HC groups (Red color edges in A). Error bars represent the standard error of the mean.

Table 1. Participant sociodemographic and clinical characteristics

| | OCD (n= 30) | SIB (n=21) | HC (n=31) | Statistics |
|--------------------------|-------------|-------------|------------|----------------------------|
| Age | 32.4 ± 10.0 | 30.4 ± 10.2 | 32.3 ± 8.5 | F= 0.323, p= 0.725 |
| Education (years) | 12.1 ± 3.9 | 12.6 ± 3.8 | 13.0 ± 4.6 | F= 0.789, p= 0.558 |
| Sex (Male/Female) | 13/17 | 8/13 | 13/18 | $\chi^2= 0.262$, p= 0.877 |
| Pack years of smoking | 3.5 ± 5.9 | 4.6 ± 8.1 | 5.7 ± 8.2 | $\chi^2= 1.295$, p= 0.523 |
| OCD age of onset | 25.0 ± 9.7 | | | |
| DYBOCS severity | | | | |
| - Aggressiveness | 6.7 ± 4.6 | | | |
| - Sex/Religion | 3.9 ± 4.6 | | | |
| - Symmetry/Ordering | 4.7 ± 4.5 | | | |
| - Contamination/Cleaning | 6.0 ± 4.8 | | | |
| - Hoarding | 1.5 ± 3.5 | | | |
| - Miscellaneous | 3.3 ± 4.4 | | | |
| - Total | 17.7 ± 5.1 | | | |

Data are presented as mean ± standard deviation. HC, healthy controls; OCD, patients with obsessive-compulsive disorder; SIB, unaffected siblings; DYBOCS, dimensional scale for the assessment of the presence and severity of obsessive-compulsive symptoms.

Table 2. FA and RD values from the significant clusters in which decreased FA and increased RD were observed in OCD patients compared to HC.

| | OCD (n= 30) | SIB (n= 21) | HC (n=31) | OCD vs HC | SIB vs HC |
|----|---------------|---------------|---------------|-------------------------|-------------------------|
| FA | 0.434 ± 0.028 | 0.456 ± 0.025 | 0.463 ± 0.024 | p = 0.033 t = 4.307 | p = 0.341 t = 0.963 |
| RD | 0.655 ± 0.038 | 0.625 ± 0.035 | 0.618 ± 0.029 | p = 0.049 t = -4.238 | p = 0.466 t = -0.737 |

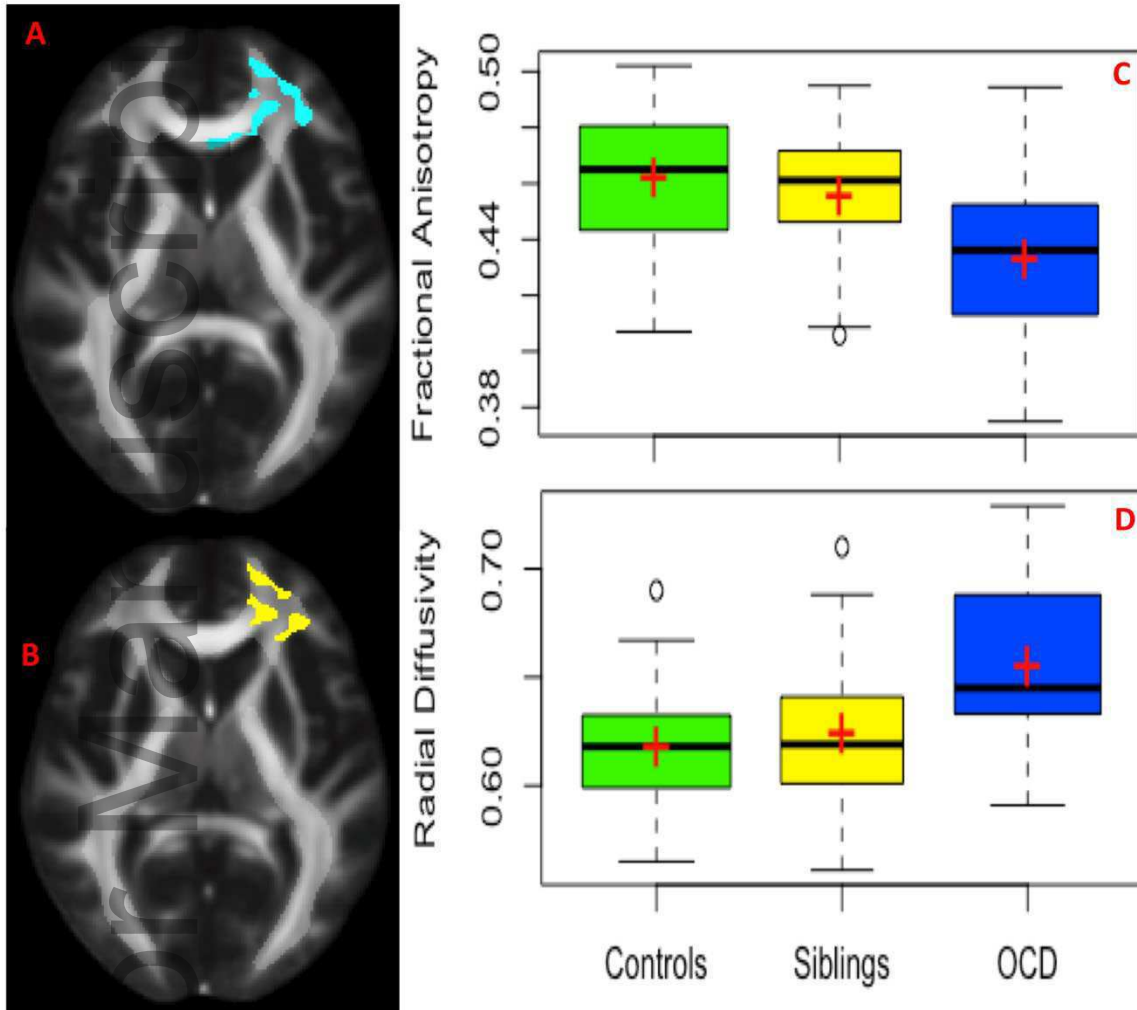
Data are given as mean (standard deviation). HC, healthy controls; OCD, obsessive-compulsive disorder; SIB, unaffected siblings; FA, fractional anisotropy; RD, radial diffusivity; RD: $\times 10^{-3}$ mm²/s.

Author Manuscript

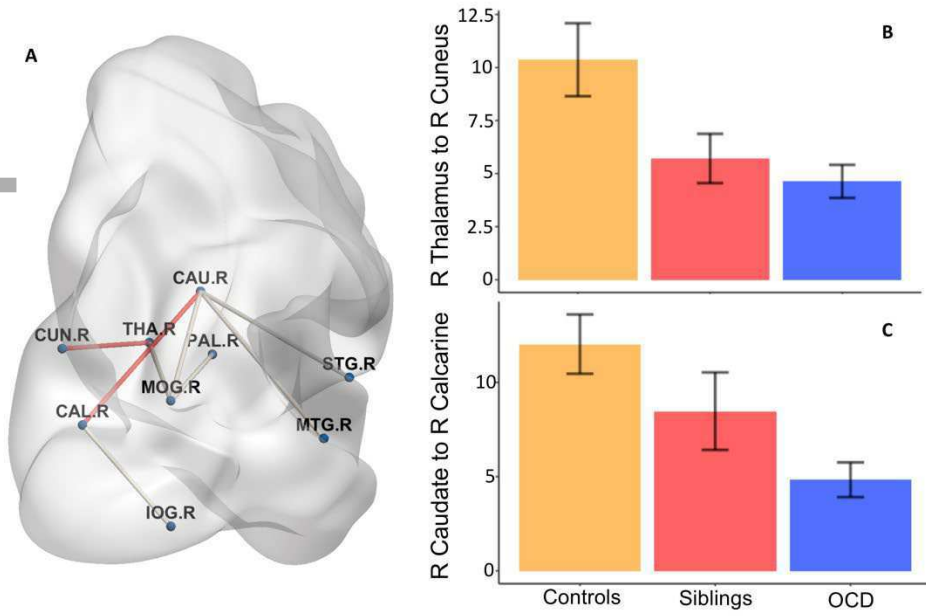
Table 3 Decreased streamline counts in OCD patients compared to HC

| Network edges | | OCD vs HC NBS t-statistics | SIB vs HC (uncorrected level) |
|---------------|-----------------------------------|-------------------------------|----------------------------------|
| 1 | R Caudate to R Temporal Middle | 3.76 | p = 0.365 |
| 2 | R Caudate to R Temporal Superior | 3.31 | p = 0.302 |
| 3 | R Caudate to R Calcarine | 3.87 | p = 0.043 |
| 4 | R Caudate to R Occipital Middle | 4.20 | p = 0.406 |
| 5 | R Thalamus to R Cuneus | 3.64 | p = 0.019 |
| 6 | R Thalamus to R Occipital Middle | 4.03 | p = 0.118 |
| 7 | R Pallidum to R Occipital Middle | 3.32 | p = 0.307 |
| 8 | R Calcarine to Occipital Inferior | 3.71 | p = 0.731 |

Author Manuscript



Author Manuscript





Minerva Access is the Institutional Repository of The University of Melbourne

Author/s:

Dikmeer, N; Besiroglu, L; Di Biase, MA; Zalesky, A; Kasal, MI; Bilge, A; Durmaz, E; Polat, S; Gelal, F; Zorlu, N

Title:

White matter microstructure and connectivity in patients with obsessive-compulsive disorder and their unaffected siblings

Date:

2020-10-22

Citation:

Dikmeer, N., Besiroglu, L., Di Biase, M. A., Zalesky, A., Kasal, M. I., Bilge, A., Durmaz, E., Polat, S., Gelal, F. & Zorlu, N. (2020). White matter microstructure and connectivity in patients with obsessive-compulsive disorder and their unaffected siblings. *ACTA PSYCHIATRICA SCANDINAVICA*, 143 (1), pp.72-81. <https://doi.org/10.1111/acps.13241>.

Persistent Link:

<http://hdl.handle.net/11343/267321>

File Description:

Accepted version